Spectroscopy 17 (2003) 323–344
IOS Press

Fibre-optic IR-spectroscopy for biomedical diagnostics

Uwe Bindig [a,*], Ingo Gersonde [a], Martina Meinke [b], Yukiyo Becker [a] and Gerhard Müller [a,b]

[a] *Laser- und Medizin-Technologie GmbH Berlin, Fabeckstr. 60-62, 14195 Berlin, Germany*
E-mail: medtech@lmtb.de

[b] *Univ.-Hosp. Benjamin Franklin, Freie Universität Berlin, Institute of Medical Physics and Laser Medicine, Fabeckstr. 60-62, 14195 Berlin, Germany*
E-mail: lmzwe19@zedat.fu-berlin.de

Abstract. The use of microscopy is a valuable means of gaining vital information for medical diagnostics. Due to a number of recent technological developments advances have been made in IR microscopy and in particular, rapid detection methods. Microscopic examination methods usually involve sampling followed by a method of sample purification or preparation. The advantages of the IR analytical method are that it is based on a direct, non-destructive measurement of sample material and that the resulting IR spectra provide extensive and specific information about the sample composition and structure. The course of a disease can lead to either formation or loss of organic compounds in metabolism as well as changes within the biological matrix. Corresponding changes can also be expected in the IR-signature in view to the grading of alteration. Our preliminary IR microscopic investigations compared diseased and healthy tissue samples individually and basic information was obtained about the tissue specific spectral signature, taking account of biological variance. Human tissue samples taken from the colon were used for these studies. Given the number of endoscopic applications used in minimally invasive medicine, we hope to establish the IR fibre based procedure as an optical biopsy method for tissue diagnostics. The aqueous environment as well as the IR radiation source, signal detection and the flexible wave guide type will be a limiting factor for an IR system. The hygiene requirements are particularly high for a fibre based system to be used for *in vivo* applications.

First experiments were used to check the transmission of the IR microspectroscopic data. Fibre supported measurements were made in ATR and remission. High powered IR laser diodes were tested in subsequent trials for application in biomedicine. First results are presented on the way to an IR-endo-spectroscopic system.

1. Introduction

Over the last decades the development and design of cylindrical optical fibres made of flexible quartz wave guides, has been offering many new applications and new technologies in the medical field. For example the development of laser assisted endoscopy in minimally invasive medicine is based on to the application of efficient and powerful light guide systems. Flexible fibres provide an useful technique for the topical non-invasive medical diagnostics. Consequently this leads to minimize the patient pain and an overall cost reduction.

IR-spectroscopy is a non-destructive, rapid and sensitive optical method, which is mostly used for analytical purposes. Routine measurement modes are transmission, reflectance and ATR (attenuated total reflectance). Optical fibres transparent in the mid-infrared (IR) make it possible to carry out absorption measurements at a remote location. IR fibres can be used for measurements in the remission and ATR-mode. If the IR-fibre is in contact with a sample that has characteristic absorption lines, the total

*Corresponding author: Tel.: +49 30 8449 2326; Fax: +49 30 8449 2399; E-mail: U.Bindig@lmtb.de.

transmission of the fibre and sample will decrease at these lines. This can be utilized to determine the absorption of a sample in a non-destructive manner.

It has been found that normal tissues exhibit absorption spectra different from diseased tissues, and it can be assumed that each diseased state of biological tissue has its own distinct characteristic IR spectral pattern [1,2]. However, marked differences can be found between the methods of sample preparation in terms of the measuring mode, the measured parameters and the conditions of the sample. In order to avoid artifacts origin by the sample preparation, fibre-optic methods should be recommended. An IR fibre-optic sensor can be inserted through a biopsy needle or a catheter and measurements can be carried out in real-time. This will permit visible information and IR-spectroscopic data to be combined in both minimally invasive medicine (endoscopy) and open surgery.

In the mid-IR range polycrystalline silver halide fibres are preferred to chalcogenide or fluoride glass fibers, e.g., TAS (Te–As–Se) wave guides [3,4]. The former are particularly suitable because of their transparency in the infrared and in their physical properties, namely they are non toxic, flexible, non-hygroscopic, low optical attenuation and have a long term/time stability. New techniques and modifications to the fibre typ, material, geometry, shape and coating extent the range of applications, so that IR fibres can be used as biosensors [5–11]. This may be attractive because their use does not require any specific expert knowledge although they do provide accurate findings with samples that have been treated not at all or minimally, only.

Some possible applications in medicine and pharmaceutics have been published which are based on fibre-optic mid-IR-spectrometry [12–14]. For example Katzir et al. [15] have designed a special measuring cell for an IR-spectrometer which is equipped with a silver halide fibre to analyse blood serum; Artjushenko et al. [14] as well as Butvina et al. [16] have used IR-fibres for the detection of melanoma and other skin diseases. This was also described by Bruch et al. [17] where they have used the Fourier transform infrared evanescent wave (FTIR-FEW) spectroscopy for the spectral characterization. Acupuncture points on human skin were investigated too [18]. Attempts were made by Wu et al. using chalcogenide fibre-optic techniques to distinguish malignant from normal oral tissues and for diagnosis of cancer [19, 20]. However lead salt diode laser which have been used for gas analysis [21,22] may give the opportunity to enhance the sensitivity of detection for monitoring and diagnostics of tissue.

Currently there is no routine clinical application which uses IR-sensors. We have focused our attention on the biomedical application of IR-spectroscopy for diagnostics purposes such as the detection of changes within biological tissues. This method may even be used for the real time monitoring of coagulation processes or on-line diagnosis of different bio-fluids.

This paper describes the experiments which were conducted on bio-gel, micro-organism and colon tissue using either FTIR-spectrometer together with fibre-optic IR-sensors or IR-microscope. Silver halide fibres were used to carry out ATR and reflection measurements (Fig. 1). The technical design of the laboratory set up and outcome of the developments for the utilization of IR laser diodes as radiation source will be discussed. In this work we report on our efforts to develop an infrared method to differentiate between diseased and healthy tissue *in vitro*.

2. Method

Micro-FTIR-measurements were performed in transmission, ATR (micro-ATR objective, Germanium, area of contact $100 \times 100\ \mu m^2$) and remission mode. Two Fourier Transform Infrared (FTIR) interferometers (each Series System 2000, PerkinElmer, USA) were used. One equipped with an IR-microscope

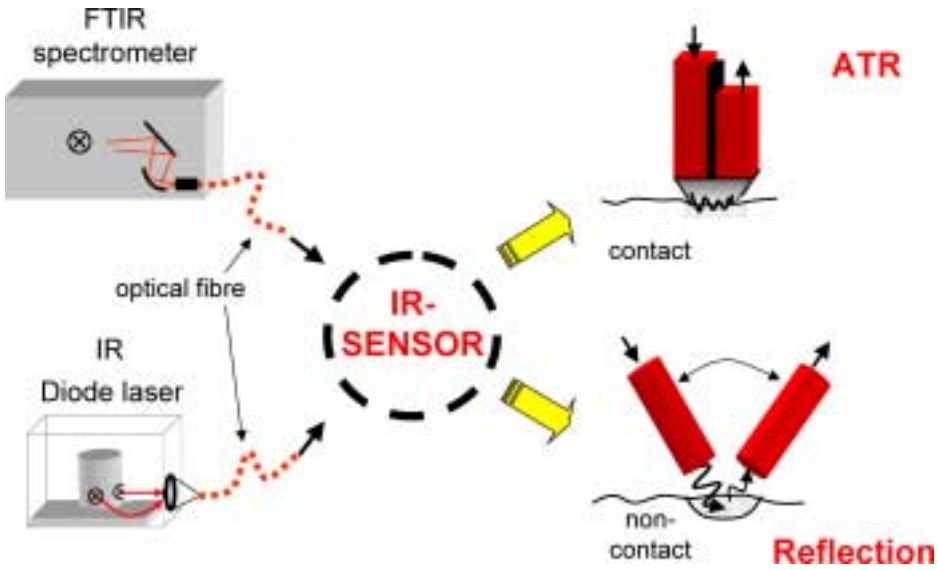

Fig. 1. Scheme for a fibre-optic set-up.

(AutoImage, PerkinElmer, USA) including a CCD-camera for the visible range and the other with the fibre-optic set-up. MCT (Mercury-Cadmium-Telluride) detectors were used for recording spectra. Data analysis was performed by the Image Data Collection Software (Perkin Elmer, USA) and self-made software.

2.1. IR-microscopy

Human colon tissue specimens were made available by the Institute of Pathology, Univ.-Hosp. Benjamin Franklin, Freie Universität Berlin, Germany. Fresh, native specimens of healthy and malignant tissue were investigated from the same patient. No fixation or freezing media were used to avoid artefacts or alteration of the specimens. Native 10 μm thin tissue cryo-sections (Microm, Germany) were transferred to calcium fluoride slides (spectroscopy central, UK) and air-dried which reduced the average thickness of the tissue sections to 2–3 μm. The specimens were stored in dry, darkened conditions at room temperature until these air-dried tissue sections were used for IR-measurements. The stability of the IR-spectra was confirmed periodically, only slight shifts then being observed in the signal intensity. After visual and IR-spectroscopic mapping, each sample was stained with hematoxylin–eosin (HE) and assessed by a pathologist.

The measurement was standardized for the mapping procedure using the following parameters: areas of approx. to 3×3 mm^2 were mapped in transmission mode with a quadratic aperture of 100×100 μm^2 and a step width of 100 μm. Each IR-map has up to 900 spectra in the spectral range of 4000–900 cm^{-1}, a spectral resolution of 6 cm^{-1}, data interval 2 cm^{-1}; apodisation: Filler, 16 scans were co-added. After every 5 measuring points a new background was scanned to compensate for the influence of carbon dioxide and water vapor. A visible image of the mapped area was taken for the native sample and then after staining. The images were compared to check for possible distortions caused by the staining procedure. The overlay error has been found to be less than 5 μm. In doing this, the pathological assessment of the stained section enables a classification of the IR-spectra according to tissue type and cancerous versus normal tissue. An initial assessment of parallel, thin HE-stained tissue sections was carried out by the

pathologist using standard histological parameters. The data obtained represents the basic information required for carrying out FTIR-spectroscopy measurements. The native section was stained after the IR-mappings were complete to enable direct comparison with the resulting IR-image. After the pathologic assessment, analysis of the IR-data followed.

For bio-gel preparation, gelatine (Merck, Germany) was dissolved in distilled water by gentle heating which resulted in a homogenous, opaque gel obtained after cooling. Micro-organisms preparation: suspensions of 3T3 fibroblasts (embryonal mouse) or CX1 (human adenocarcinoma of the colon) were concentrated carefully by centrifugation (Labofuge, Heraeus, Germany), washed two times with distilled water and concentrated again. Rapid freezing (liquid nitrogen) of the precipitate leads to a pellet.

2.2. Fibre-optic measurements

Fibre measurements were carried out in ATR and remission mode. Parameter were set as follows: 32 scans were co-added; spectral range 2600–800 cm^{-1}; resolution 4 cm^{-1}; apodization strong. An external pigtail MCT-detector (sensitive area 500×500 μm^2) equipped with an internal pre-amplifier (Infrared Fiber Sensors, Germany) and a MCT-detector (Graseby, USA) was used for spectral detection. A laboratory-made system was used for the in-coupling of the IR-radiation: a SMA-connector was positioned directly in the path of the internal DTGS- (deuterated triglycerine sulphate) infrared detector. A selection of non-human tissue specimens were even used for the fibre-optic measurements. To avoid reflectance of IR-radiation from a deeper interface or from the reverse side of the sample the native tissue thickness was set at >400 μm for the fiber-optic measurements.

Polycrystalline circular silver halide fibre were used: 1–1.5 m length, core/clad: 700/900, NA 0.6 (Infrared Fiber Sensors, Germany) and MIR-860/1000 (Institute of Advanced Fiber Optics, Russia).

ATR-measurement: (a) IR fibre sensor: an ATR-sensor device (Infrared Fiber Sensor, Germany) and prefabricated circular fibres and (b) an IR-sensor: quadratic polycrystalline silver halide fibres 750/750 μm^2, NA 0.6, length 1.75 m (Infrared Fiber Sensors, Germany) which were connected to a sensor tip (diamond prism, rectangular spot 1.5×2.5 mm^2) were used.

Remission measurement: (a) distal ends of the fixed excitation- and detection-fibre were brought at an angle of incidence of 60° near each other, the fibre to tissue distance was approx. 0.5 mm; (b) remission sensor (Infrared Fiber Sensor, Germany), each fibre is fixed in a teflon holder. A gold standard was used for the background measurements.

2.3. Lead-salt diode laser

A tunable diode laser source module TLS 212 equipped by two multimode lead-salt diode lasers (cooled by liquid nitrogen) and two TSL 150-1A laser controller (current and temperature) was used (Mütek Infrared Systems, Germany).

3. IR-microspectroscopy

3.1. Bio-gel

To simulate the optical properties of tissue in the infrared region, gelatine was used as phantom. The main component of gelatine is the biopolymer collagen which causes a three dimensional network of bundles within the matrix. To simulate scattering effects due to micro-structures and even for moist

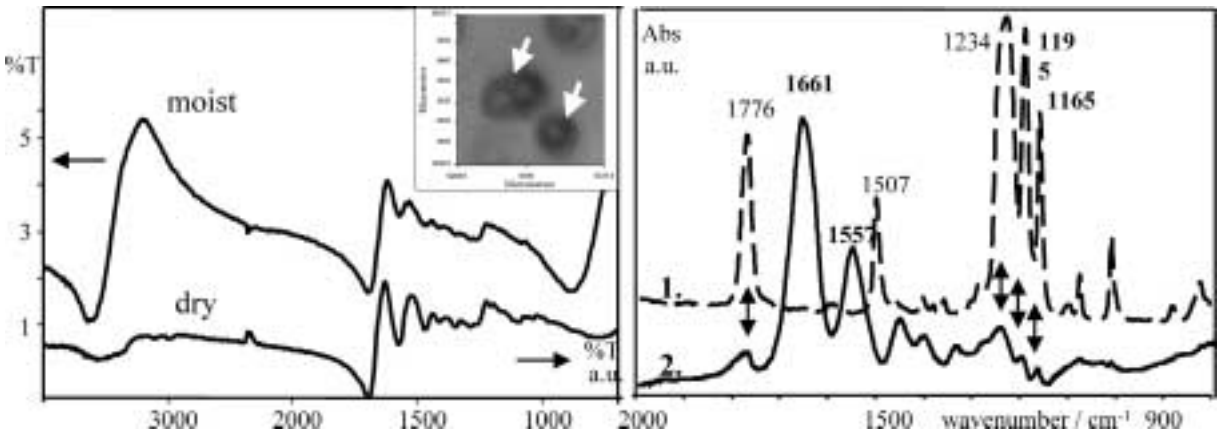

Fig. 2. On the left, reflection spectra (IR-microscope) of moist and dry gelatine including scattering particles; inset, visible image of polystyrene micro beads in gelatine matrix (diameter 11 μm). On the right, IR-reflection spectra after Kramers–Kronig conversion, (1.) the polymer slide, (2.) a 250 μm thick gelatine section on the polymer slide.

tissue practical applications, investigations were carried out using polystyrene particles suspended in gelatine using the IR-microscope in reflection mode. The diameter of the polystyrene beads was set in accordance to the averaged diameter of fibroblasts. Further to investigate the penetration depth of the infrared radiation cryo-sections of the freshly prepared bio-gel were mounted on to polymeric slides.

In result, Fig. 2 shows IR-remission spectra of moist and dry gelatine with scattering particles. The spectra indicates an enhanced signal intensity of the dry gelatine specimen in the spectral region >1700 cm^{-1}. No affects could be observed due to the scattering properties of the sample, while there are no additional absorption bands. A strong remission was detected using a blank polymeric slide and a slide covered by a moist 250 μm thick gelatine (10%w/w) section. The band intensities observed are due to the specular reflectance which is caused by the smooth surface of the specimens. The absorption bands at 1661 and 1557 cm^{-1} are assigned to amide I and II. There are also some minor absorptions bands which can be attributed to the polymeric slide. In this way it was possible to estimate the penetration depth of the IR-radiation.

3.2. Micro-organism

A simple biologically relevant system was selected prior to the IR spectroscopic investigations on complex tissue. For this purpose IR maps of 10 μm thin sections of pellets of relevant cell culture lines (CX1 and 3T3 fibroblasts) were investigated with the IR microscope both separately and mixed (CX1 : 3T3 = 1 : 10). Initially IR mean spectra of the cells were generated, compared to each other and the correct allocation in the IR map checked. No synchronized cell lines were used for the measurement. Supposing an average cell diameter of 10 μm, one pixel in the IR map (aperture 100×100 μm^2) contains approximately 127 cells, the information of which correspond to one IR spectrum. In result the 3T3 fibroblasts which roughly correspond to connective tissue do not show any foreign bodies in the IR map (not shown). By contrast in the IR map of the CX1 cells minimally false allocations can be seen. However the IR map of the artificial cell mixture shows both of the cell lines in approximately the correct proportions. Results of the data analysis are shown for black and white assignment in Fig. 3.

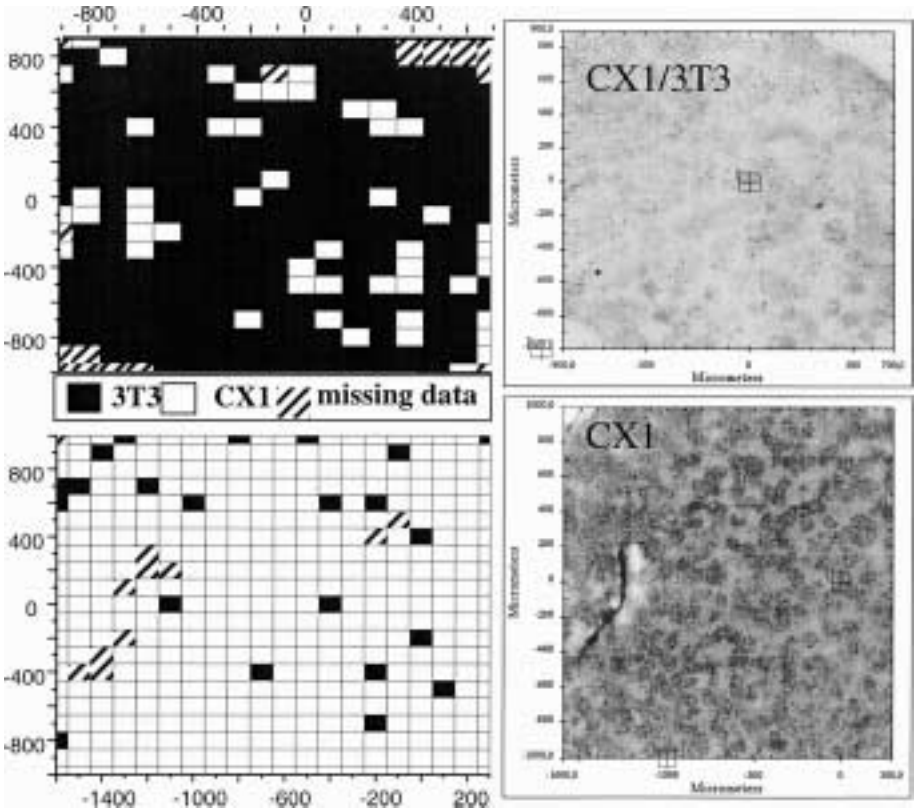

Fig. 3. Visible images of the native or post-HE-stained pellet sections, and the corresponding maps from the data evaluation using IR-mean spectra (wavenumber range 4000–900 cm^{-1}).

3.3. Tissue

The following sequence was applied to each sample for analysis of the IR microscopic data:

(1) a visible image and (2) an IR-map of the non-stained section was made and a grid was set to the image according to the mapping aperture; (3) the native sample was HE-stained after the measurement (the grid was used for exact relocation of the sample on the instrument); (4) finally, a pathological assessment was made according to the image of the HE-stained section together with the classification of each IR-spectrum with regard to tissue type. For exact assignment (Fig. 4) the pixels (100×100 μm^2) were only used if the certainty of classification was 100%. This allowed the corresponding IR-spectrum to be correlated with the histological image. With the classification of most of the spectra it is possible to use statistical methods to differentiate between different tissue types.

Correlation coefficient analysis, multivariate and univariate discrimination analysis (LDA, QDA) were uses for data evaluation. With respect to the use of IR laser diodes a discriminatory analysis method was used in which the evaluation of the spectra was limited to two wavenumber ranges ($\Delta\nu$ max. 50 cm^{-1}). From the data of these ranges, one quotient was derived for one each spectrum, that proved to be invariant for linear scaling of the spectrum. The quotient was determined by the univariate QDA. The position of the wave number ranges or the data considered within these ranges were optimized by means of a genetic algorithm, thus minimizing the error quota of the QDA [23–26]. The optimization yielded several solutions with comparable discrimination capacity. The wavenumber range from 1220 to 1240 cm^{-1} is

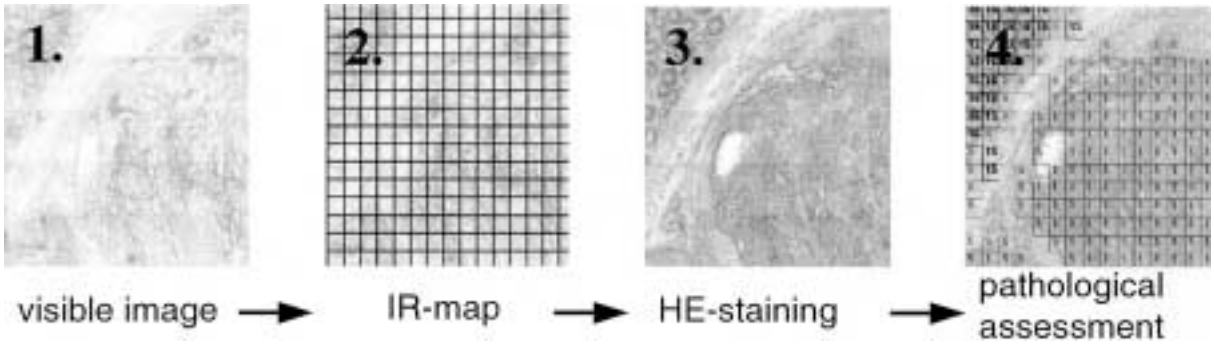

Fig. 4. Typical sequence used for the IR-microscopic specimen analysis.

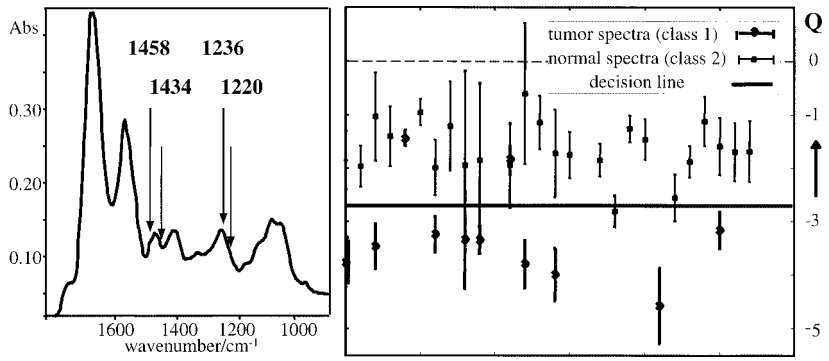

Fig. 5. On the left: position of the wavenumber in the tissue spectrum for the calculation of Q in (a). On the right: distribution of the quotients (b) in 26 IR maps; black: mean and standard deviation of Q based on the tumour spectrum of one map; grey: values based on the spectrum of a map for normal tissue samples. Spectra from class 1 with values of Q over the decision line would be classified as false negative, spectra from class 2 with values below the decision line would be classified as false positive.

involved in most solutions.

$$\text{(a)}\quad Q = \frac{A(1458\ \text{cm}^{-1}) - A(1434\ \text{cm}^{-1})}{A(1236\ \text{cm}^{-1}) - A(1220\ \text{cm}^{-1})}, \quad \text{loss} = 4\%,\ \text{contamination} = 6\%,$$

$$\text{(b)}\quad Q = \frac{D^{(1)}[A](1446\ \text{cm}^{-1})}{D^{(1)}[A](1224\ \text{cm}^{-1})}, \qquad \text{loss} = 4\%,\ \text{contamination} = 10\%.$$

The error indications for the two optimised quotients refer to validation by re-substitution by 26 IR maps. In (a), four absorption values are used for the calculation of Q. Figure 5 shows their position in the fingerprint region of the tissue spectrum. In (b), $D^{(1)}[A](\nu)$ signifies the finite-difference approximation of the first derivative of the spectrum, which is formed by means of five equidistant absorption values around the wavenumber. Figure 5 gives an example for the distribution of quotient (b). The difference between the mean values of each map is in sometimes greater than the standard deviation within individual maps This shows that the variance between the biopsy samples contributes considerably to the errors in the discriminant analysis.

Figure 5 shows examples of the wavenumber range (b), the 1st derivative at 1446 and 1224 cm^{-1}. The images resulting from this evaluation method are generally black and white. To gather some addi-

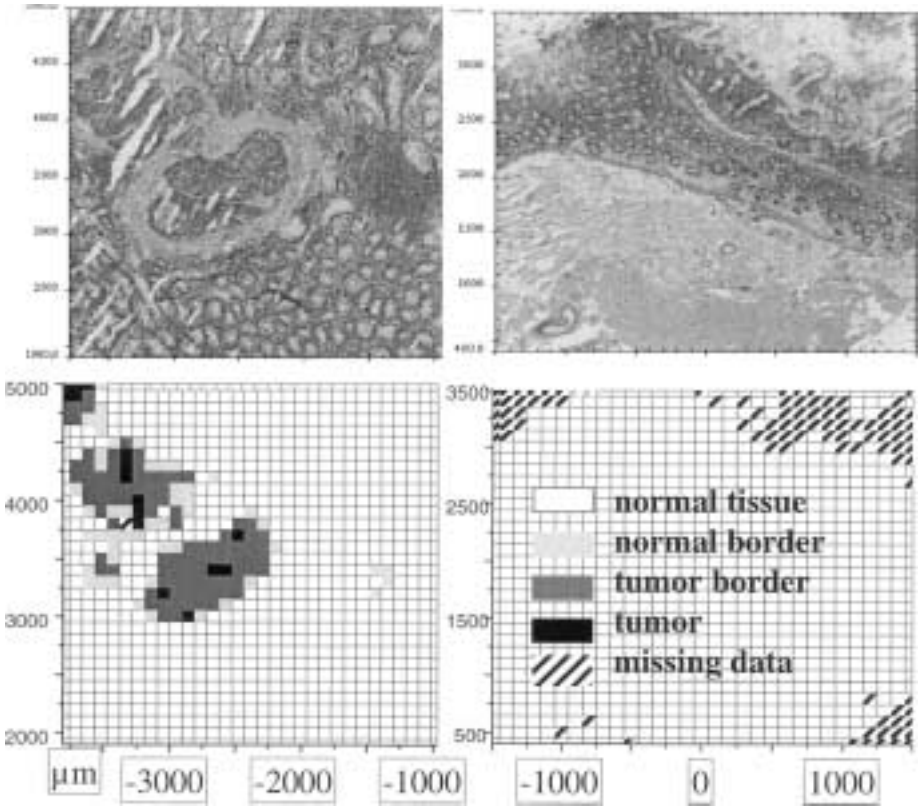

Fig. 6. Above: microphotograph image of the post-HE-stained tissue sections (left/tumour and right/normal). Below: corresponding evaluation using the wavenumbers 1446 and 1224 cm^{-1}.

tional information for the first results, a border region between the tumour and the healthy tissue was defined extending to $\pm 10\%$ of the distance between the mean values and being symmetrically around the limit value. This way two additional grey tones are obtained. It can be visually observed whether or not the determined quotient values are close to the tumour-to-healthy-tissue limit value. Consequently, the distribution in the border region can be controlled from case to case. Figure 6 shows a tumorous thin tissue section, which was not used for calibration. In the left section, medium to top, the tumorous tissue is visible, to the right a lymph node can be seen, which is classified as being non-tumorous. In the bottom of the image, non-tumorous crypts are visible. The tumour is distinctly differentiated from the non-tumorous tissue. The thin tissue section of the non-affected tissue is represented as a white area with hatched sections, inside which the IR spectra could not be evaluated. Similar to the result of the pathological evaluation, no tumour was recognised here. Cryo-sections of healthy tissue are frequently represented as white areas with missing data points, only, if any. This methods provides no information on the kind of tissue, there is only a differentiation between the tumour and the healthy tissue.

All assignment-based methods depend on the classification and cannot be better than the pathologist's classification. Any errors, which may happen due to that assignment, will be reflected in all evaluation methods [2]. Therefore, an additional evaluation of the tissue sections by independent pathologists is required to provide reliability for the calibration of the method in clinical application.

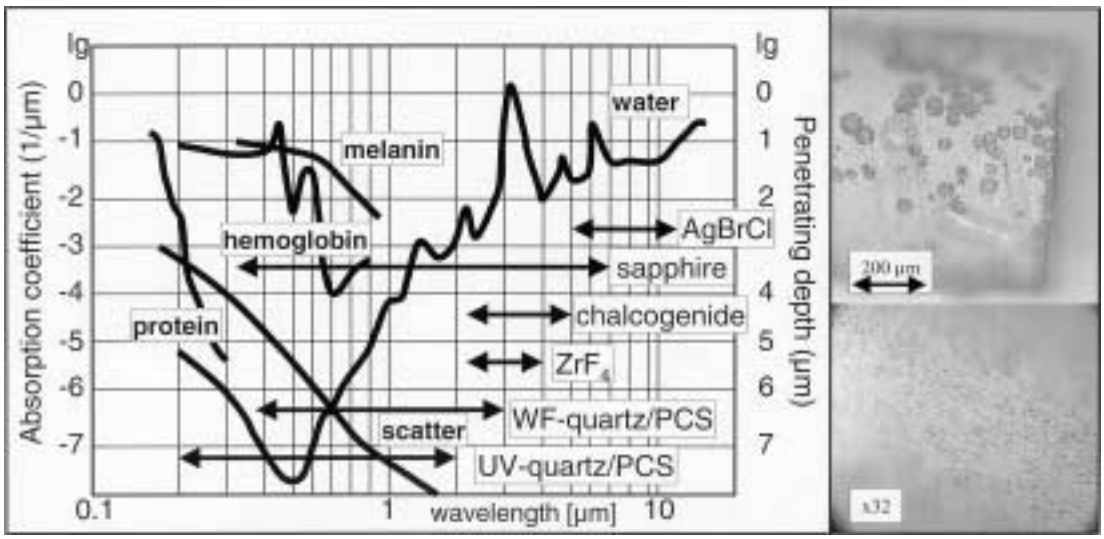

Fig. 7. On the left: simplified absorption of medical relevant bio-components and the transmission range of different wave guides. On the right; microscopic images show an altered silver halide fibre surface. Note the presence of micro-crystalline contamination.

4. Fibre assisted FTIR-spectroscopy

The use of spectroscopy in endoscopy relies on fibre optics for transmission of IR-radiation to and from the sensor at the distal end of the endoscope. We used polycrystalline silver halide fibres for our experiments because of their highly suitable spectral wavelength range and their physical properties. They are, in contrast to the chalcogenide fibres, more sensitive in the fingerprint region and have the added advantage of being ductile. Silver halide fibres are also non-hygroscopic and non-toxic. For wavelengths in the fingerprint region an attenuation of 0.2 to 0.5 dB/m are given, which means that fibre lengths of several metres are possible in clinical use. New techniques for the silver halide fibre manufacturing reported by Küpper et al. [8] will determine a reduced sensitivity for UV-radiation. The main disadvantages of chalcogenide glass fibres, such as TAS-fibres (Te–As–Se), is their low level of flexibility, a limited wavelength range for the IR-transmission and the toxicity of the material which restricts medical use. Highly flexible hollow wave guides which are transparent in the infrared range due to their internal metal coating cannot be used because they are sensitive to bending and the resulting loss in intensity has a negative affect on the IR-spectrum [27]. On the other hand even silver halide fibres can be irreversibly destroyed when brought into close contact with metal surfaces or liquids contaminated by water soluble metal salts. In the transition area fibre/connector differences in potential can lead to contact corrosion and destruction of fibre material (Fig. 7). To prevent this occurring the fibres are surrounded by a plastic coating (Teflon or polyetheretherketone – PEEK).

The following sensory units were used with the FTIR spectrometer or with laser diodes as illumination source. The transmitted power from the sensor was measured with an MCT detector.

Only a fraction of the total irradiation of the FTIR spectrometer can be coupled into the fibre (Fig. 8). This is because the effective area of the IR source in the spectrometer is equivalent to the J-Stop-aperture of the interferometer which is considerably larger than the cross section of the fibre. The projection of the light source area on the end surface of the fibre is only possible with limited reduction so that the end surface of the fibre is illuminated. Using zinc selenide lenses and an elliptical mirror the in-coupled

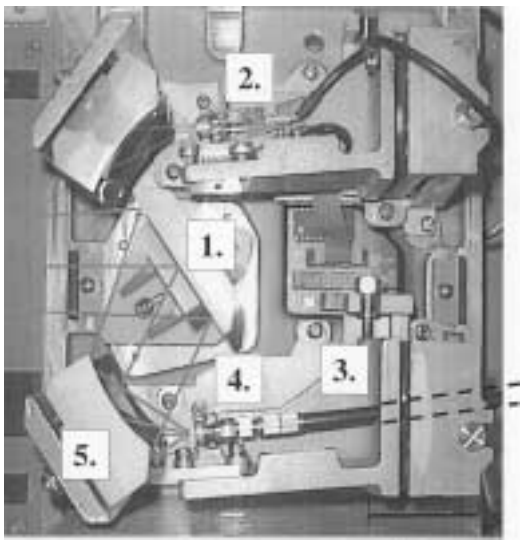

Fig. 8. Detector compartment in FTIR-Spectrometer S2000 with two detector fixtures (2. indicates the TGS-detector). In the lower mount the detector is replaced by a SMA coupler (4.) fixed to the IR wave guide (3.). The IR radiation emerging from the sample compartment is passing via a plane mirror (1.) and focussed by means of an elliptical mirror (5.) on the fibre end.

power was increased by 2 to 3 times that of normal lenses. The proportion of the in coupled power was less than 0.5% for all variations.

The in-coupling losses are the main reason for the reduced signal/noise ratio in fibre based measurements in FT-IR spectrometry. The radiation from laser diodes, by contrast, can be coupled into the fibre with a relatively small loss of intensity. ATR and reflection methods are relevant alternatives for *in vivo* use of IR spectroscopy.

4.1. ATR-measurements

4.1.1. IR fibre sensor

In addition to the transmission of IR radiation, silver halide fibres can also be used for ATR measurements. The sample is brought into direct contact with the fibre this is called fibre optic evanescent wave spectroscopy (FEWS). Using this material it is possible to realize relatively simple and small sensors.

Use with biological substances, particularly proteins, presents problems with contamination. The component material of the silver halide fibre reacts with sulphur containing compounds (thiol, disulfide, etc.) to form silver sulfide containing organic components. A discolouration of the fibre indicating this change is accompanied by an immediate worsening of the fibre transmission properties. The implementation of water molecules inside the fibre material alters the structure and will change the spectral transmission too. After the measurement has been completed and the fibre cleaned, a change can be determined in the base line spectrum. In order to avoid premature irreversible damage to the fibre we use an IR fibre sensor which allows the fibre piece used for the measurement in contact mode to be replaced (Fig. 9). The replacement U-shape circular fibre piece is connected with a plug connection to the fibres which transmit the IR radiation. Comparative measurements have shown that the plug connection of two fibres results in a 60% loss of radiation. Theoretically the losses due to reflection are normally expected to be of the order of 15 to 25%. This means that the two plug connections at the fibre head result in a loss of

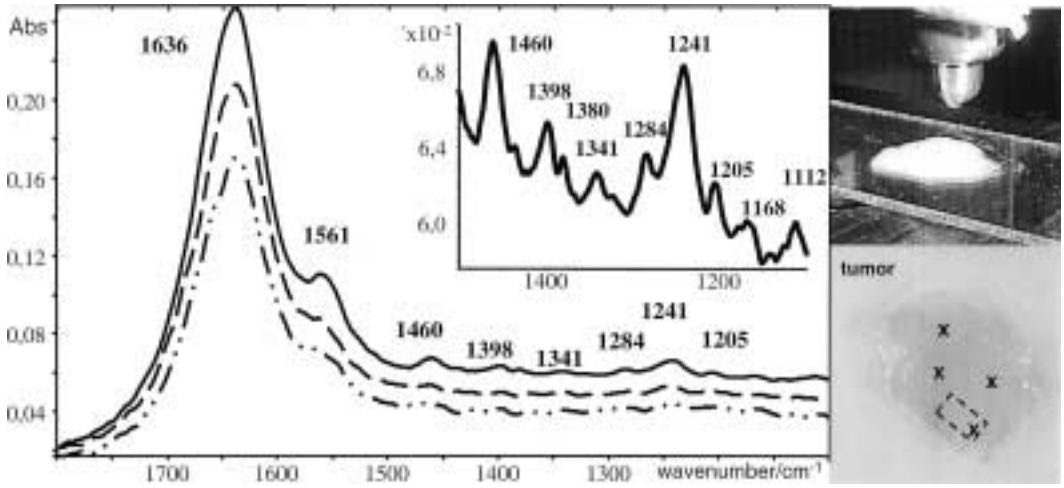

Fig. 9. IR-spectra (fibre sensor) at different measurement points (z-axis constant); inset: expanded IR-spectrum in the wavenumber range 1500–1100 cm^{-1}. Right; above, the fibre sensor head; below, photo of the native colon tissue samples after the measurement (measured points are marked with x).

90% of the IR transmitted radiation. Connected to the FT-IR spectrometer a relatively small signal/noise ratio of 30–130 in the fingerprint range (1800–900 cm^{-1}, resolution 6 cm^{-1}, one scan) is achieved.

The contact area between the bent fibre and a tissue sample varies according to the pressure applied to the fibre. The amplitude in the absorption spectrum changes accordingly. When samples are covered with a film of water the fibre is wetted where there is contact leading to a tissue spectrum overlaid with an over proportional water signal. In order to avoid this effect a plastic layer or coating around the fibre in the measurement area is advantageous whereby a defined measuring area can be kept free. A polymer covering (μm thickness) on the area to be measured can also help to reduce the contamination of the fibre. Relevant coating experiments have been carried out by Bormashenko et al. [28] and others [29].

Human tissue samples measurements were carried out on a glass and/or polymer slide with a stepwise motor drive positioned below the sensor head. The samples were moistened at regular intervals with physiological saline solution. Prior to the IR measurements 10 μm thin tissue sections were cut from the tissue block and analysed spectroscopically in transmission. The silver halide fibres were cleaned before every measurement and a background spectrum was taken. Photographs were taken after the fibre sensor measurement for the documentation of the tissue conditions.

An example is shown in Fig. 9, the total sample area was 11×9 mm^2 for tumorous and 12×10 mm^2 for healthy. The determined sample thickness was 3–4 mm.

The handling of the samples proved to be difficult due to the consistency of the colon tissue (tissue mechanics/deformation). Tissue stuck to the fibre and had to be carefully freed. This happened particularly on the superficially dried colon tissue. The sample was first measured by placing the fixed IR fibre sensor directly on the sample. Directly after this the sample was placed under an IR microscope and the procedure was repeated at the same points. The IR-spectra of the sensor procedure vary greatly from one another with regard to the absorption intensity (z-axis constant, see Fig. 9). This effect is a result of the tissue specific mechanics which lead to a non-homogenous tissue topography. The tissue ‘evades’ the IR fibre, at the same time the contact area tissue/fibre increases. Typical absorption bands for proteins were observed, i.e., amide-I and II-bands. The intensity of the IR absorption is shifted dependent on the fibre sensor handling, i.e., by pressing it onto the tissue surface at the same area (not shown). As conse-

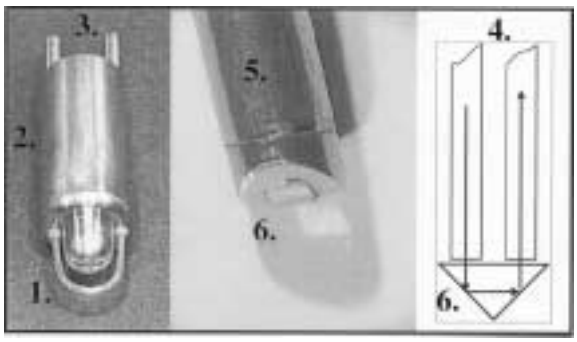

Fig. 10. ATR-sensor. On the left: IR-fibre sensor, the sensor head (diameter 5 mm) with exchangeable U-shape circular silver halide fibre (total length 7 cm, diameter 700 μm) (1.), sensor body (total length 29 mm, diameter 10 mm) (2.), connectors for the silver halide cables (3.). On the middle: IR-sensor tip, square silver halide fibres for excitation and detection purpose (total length of each 1.5 m, diameter 750 $\times$ 750 μm^2) (4.) are fixed inside the metal tube (outer diameter: 4 mm) (5.) to a diamond prism (6.). On the right: scheme of the IR-sensor.

quence this leads to a more intensive contact between medium and measurement device. The different absorbance in the contact area mainly leads to a change in the penetration depth of the IR radiation. Due to effects caused by squeezing out of water from the interstitial space and/or the tissue surface a change of intensity from the amide absorption bands to the lipid absorption bands were observed.

4.1.2. IR-sensor

The IR radiation is passed through a diamond prism with two total reflections (Fig. 10). The sample to be measured is brought into contact with the prism. The deliverance (excitation and detection) of the IR radiation results through two oblong square silver halide fibres that are permanently fixed to the prism. The prism and the fibres are built into a metal tube and are hermetically sealed. The two measuring areas of the prism are 1.5×2.5 mm^2.

The transmission of the IR-sensor is very high being about 50% of the transmission of a silver halide fibre of equivalent length. In combination with the FTIR-spectrometer a signal/noise ratio of 150–600 was measured in the fingerprint range (resolution 6 cm^{-1}, one scan). After the tissue samples have been measured the diamond prism was cleaned by rinsing with water. Figure 11 shows the IR-spectra which were obtained using the diamond sensor and micro-ATR-measurements (IR-microscope) applied to moist non-human tissue specimens. Measurements were carried out at the same position on the tissue specimen. As the micro-ATR-measurement procedure has a considerable higher degree of resolution (100 μm) it would be reasonable to expect different band intensities. However comparison shows that the line forms and positions are mostly in agreement.

The scatter plot in Fig. 12 with a total of 59 measurements after PCA transformation shows that the measurement of one type of tissue for both measuring techniques lay next to each other ie are similar. This confirms the quantitative comparison in Fig. 11, according to which both measuring techniques give similar spectra.

4.2. Reflection measurements

Reflection spectroscopy is from the clinical aspect a preferential alternative to ATR spectroscopy as it is based on contact free measurement of the probe. This means that contamination of the optical elements can be avoided particularly in endoscopic use. The potential probability of tumourous tissue being spread

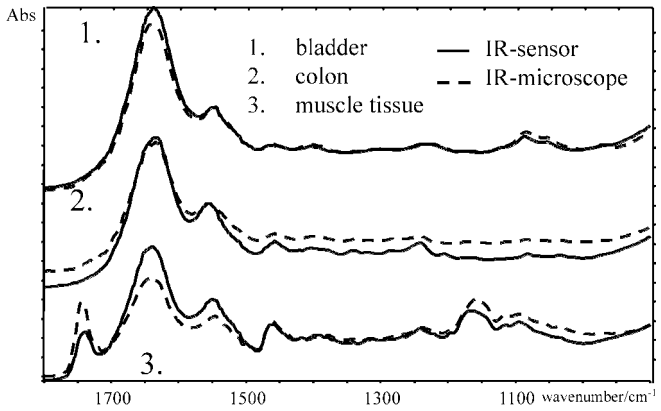

Fig. 11. Measurements with the ATR diamond sensor and micro-ATR measurement on tissue samples under moist conditions.

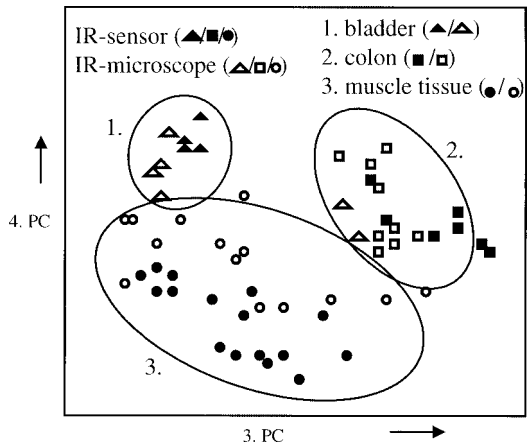

Fig. 12. Scatterplot of (3.) and (4.) principal components of 59 measurements with the ATR diamond sensor and the micro-ATR (IR-microscope). Measurements were made at different points on the tissue samples.

between the measuring points during an investigation is considerably reduced. However for fibre based measurements on biological tissue there are certain disadvantages which will be discussed below.

In principle the reflection on biological tissue is made up of two parts:

1. Fresnel reflection on the surface is for an even or sufficiently flat surface directed and for an uneven or structured surface, there are diffuse areas of reflection. The spectrum of the fresnel reflection results from the Kramers–Kronig transformation of the absorption spectrum.
2. The radiation which penetrates the tissue will be reflected by inhomogenous structures (remission). The spectrum of remission differs in its form/structure from Fresnel reflection. In some cases the Kubelka–Munk transformation can be is compared to the absorption spectrum.

Reflection measurements on fresh tissue samples were realised with a fixed illumination and a detection fibre (Fig. 13).

Due to the large angle of divergence of the radiation beam when leaving the silver halide fibre and the small fibre cross section of the detection fibre only a small proportion of the radiation is used for the measurement. At perpendicular incident radiation there is only 2% of the overall incident radiation in-

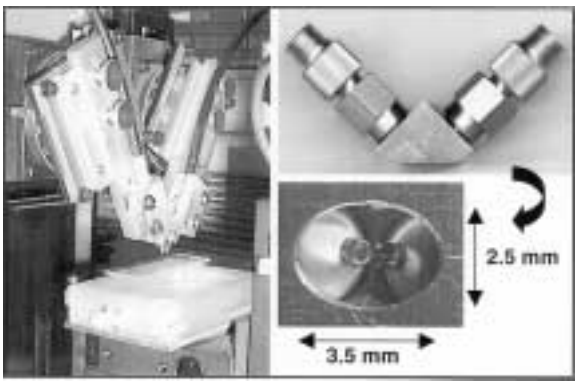

Fig. 13. Calculated IR reflection spectra for colon tissue (water content of 77%); tissue without water film and incl. water film thickness 0 to 1 μm, 0 to 2 μm and 0 to 3 μm.

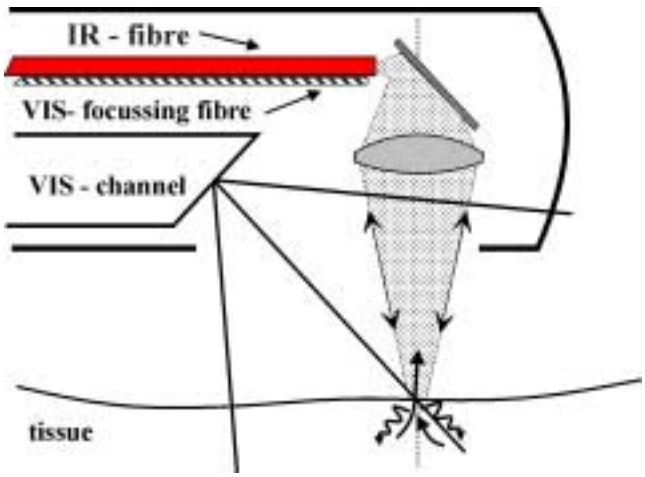

Fig. 14. Experimental prototype and set-up for the IR fibre-optic measurement in reflection mode.

tensity. Already 95% of the reflected radiation lost when the fibre end is two millimetres from the tissue. Measurement with the endoscope at a distance of approx. 2 mm due to the movement and distance dependence of the captured radiation could lead to considerable intensity fluctuations whereby a contact free measurement could not be guaranteed. The measuring distance can be stabilised with an optical spacer or IR transparency window, but then the advantage of the contact free measurement is lost. Figure 14 shows a further possiblity by which the proportion of the used IR radiation can be increased/enlarged. The emergent radiation from the illumination fibre is focussed with a lens on the tissue surface, the reflected radiation is focussed with the same lens on the end surface of the detection fibre. Ilumination and detection can be combined in one fibre. This configuration is also dependent on the tissue-side numerical aperture of the lens and if the tissue surface is not smooth, the signal intensity variation will be correspondingly high.

The tissue surface is always wet during *in vivo* measurements on biological tissue within the body. The reflection spectrum is very dependent *on the wetting/degree of wetness* of the tissue. Figure 15 shows the measurements on a muscle tissue sample that was increasingly made more wet with water. A visible

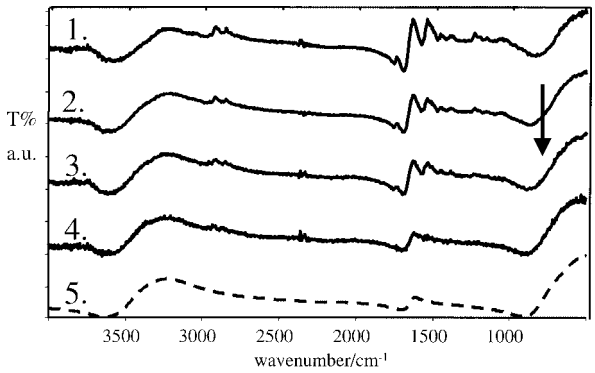

Fig. 15. Draft configuration for endoscopic reflection measurements. The IR-radiation is focussed with a lens both prior to and after reflection on tissue.

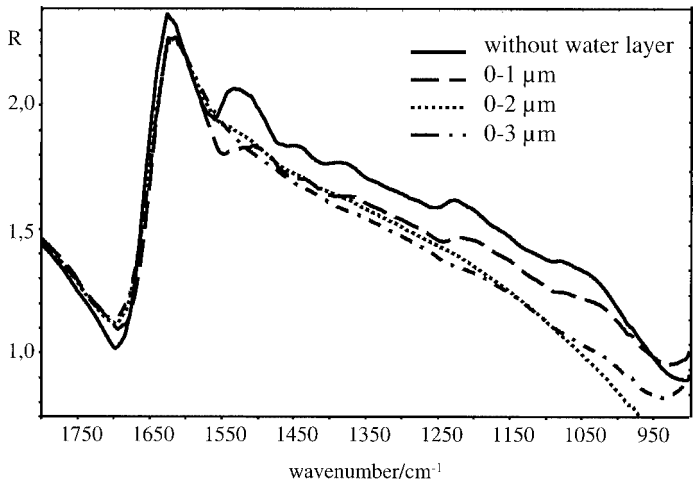

Fig. 16. IR-reflectance spectra on moist muscle tissue (bovine) with increasing water content ((1.) to (4.), (1.) a nearly dried surface, (4.) a moist tissue surface, without visible water film), (5.) specular IR reflection spectrum of water (angle of incident 30°). Spectra individually randomly normalised.

layer of water was avoided by wiping with a swab. A steady increase in the water film reduces the band intensity of the tissue, the spectrum converging with the spectrum of the water.

There is currently no quantative method available to measure the thickness of the water film. So reflection spectra on moist tissue were simulated with a water film. The frequency dependent dielectric constant of water free tissue was calculated from transmission measurement of thin sections added to the dielectric constant of water. The resulting spectra for colon tissue with a water content of 77% are shown in Fig. 16. Interference effects were avoided by averaging the water film thickness (0 – n μm).

It was found that tissue bands are already almost completely suppressed with a water film thickness of 2 μm. As a result the tissue surface must be dried before measurement when using endoscopic reflection spectroscopy. This may be realised locally without damage to the tissue with a flush of gas. The reflection signal mainly results from the fresnel reflection on the tissue surface, whereas scattering of the IR-radiation on inhomogenous structures below could not be measured.

4.3. Discussion of the measuring methods

Compared to the usual measurement of samples with the FT-IR spectrometer or transmission measurements with the IR-microscope, with the fibre based measurements it is possible to attain a significantly lower signal/noise ratio. The reason for this is mainly the high losses incurred by incoupling of the IR radiation in the fibre, together with the transition between two fibres. Table 1 summarizes the measured values obtained for stationary measurements and fibre based measurements.

The ATR measurement of the fibre based single point measurement of the tissue spectrum has the advantage of having a relatively high light yield. The transmission of an ATR sensor being almost equivalent to a wave guide without a sensor. For the reflection measurement, the tissue surface reflects approximately 2% of the incident light in the wavenumber region of interest (1000 to 2000 cm^{-1}), the light yield being correspondingly limited. Moreover the contrast of the absorption bands are reduced by $2/3$ compared to the ATR measurement (Table 2).

In the event of non-contact reflection measurement being carried out by endoscopic application, considerable intensity fluctuations are to be expected due to movement of the instruments and variation in the surface characteristics of the organ being investigated.

The IR sensor has proved useful with respect to the reproducibilty of the measurements because the polished diamond surface is inpermeable to either contamination by biological substances or chemical change and is easily cleaned. The development of a reliable connection which can be sterilised is essential for the ATR fibre sensor with interchangeable fibre. A higher radiation yield could be achieved using a set-up with a permanent continuous fibre with coating.

Table 1

S/N (signal/noise)-ratio of different measurement modes using a FTIR-spectrometer (S2000 Perkin Elmer, wavenumber range 1800–900 cm^{-1}, one scan, resolution 6 cm^{-1}, MCT-detector)

Mode	S/N-ratio	Spot
Transmission (IR-microscope)	1660–3300	$100 \times 100\ \mu m^2$
Micro-ATR (IR-microscope)	200–500	100 μm diameter
Fibre based:		
ATR-sensor tip	150–600	$\approx 1.5 \times 2\ mm^2$
ATR-fibre sensor	30–130	$\approx 0.7 \times 3\ mm^2$

Table 2

Contrast $2(A_{max}-A_{min})/(A_{max}+A_{min})$ of the ν_{as}-PO_2-absorption band at 1240 cm^{-1} in the absorptions spectrum for measurements on colon tissue samples

Measurement methods	Contrast
Transmission /dry tissue	0.5
Transmission/ATR /moist tissue	0.14
Reflection /moist tissue	0.04

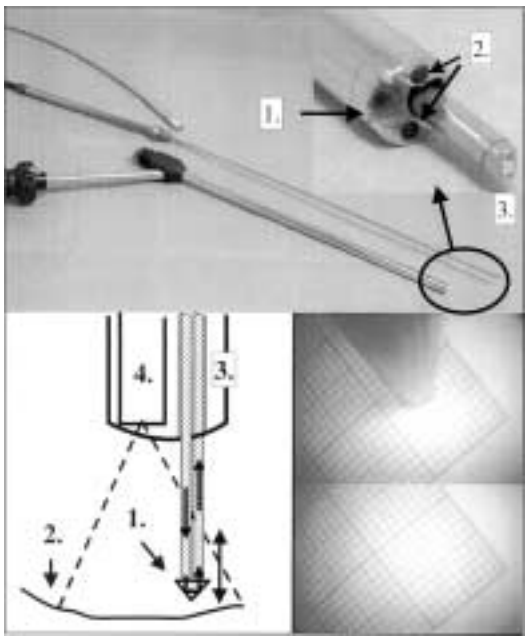

Fig. 17. Above, photograph of the rigid endoscope (lower) and IR-probe, incl. light guide coupling for the illumination in the visible; inset: distal end of the endoscope with IR-sensor in the working channel ((1.) objective, (2.) illumination, (3.) ATR-probe). Below, on the left – schematic drawing of the distal end of the endoscope with removeable IR-sensor ((1.) IR-sensor, (2.) tissue surface, (3.) working channel, (4.) visible channel); on the right – below, view through the endoscope on paper (mm-grid, working distance approx. 3 cm); above: the reeled out IR-sensor.

5. IR-endoscopy

We focussed our interest to use IR spectroscopy – which was initially tested on biopsy tissue – in a minimally invasive method for superficial tumors in endoscopically accessible hollow organs. The prototype used was the IR diamond sensor, which was integrated into a rigid endoscope. Figure 17 shows the basic set-up of the system.

The ATR-probe consists of diamond tip and the IR fibres. They are situated in the working channel of the endoscope. The moveable ATR-probe can be reeled out for the measuring. The choice of the measuring point on the surface of the organ and the positioning of the ATR sensors is aided by the monitor picture. The ATR-probe can be withdrawn from the endoscope for easily cleaning. The IR fibres on the proximal end of the endoscope are extended in flexible plastic tubes and coupled with the spectrometer.

It is important for integration into the endoscope that the diameter of the ATR-probe has the smallest possible diameter. However a measuring spot of 4 mm is necessary in order to obtain sufficient information about the status of the tissue on the tissue surface within the framework of a screening procedure (relationship cost/time involved/patient stress).

In contrast to the spectrometer, measurements with the endoscope lead to unavoidable movement of the ATR sensor and the sample. Contact of the two surfaces leads to changes in the pressure applied and the position of the tissue on the sensor, this leading to minor changes in the spectrum or the total intensity of the measured radiation. In order to simulate the measuring conditions for (real) application, manual measurements with the ATR-probe were carried out using a 2 cm thick muscle tissue sample. Figure 18 shows the temporal progression of the total intensity of the transmitted radiation. Small variations in the position of the probe resulted in intensity fluctuations of up to one percent.

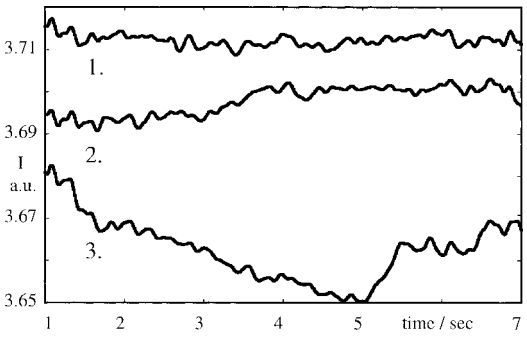

Fig. 18. Fluctuations in the signal intensity of three manual measurements on muscle tissue (pork) with the ATR-probe.

The measurement time for the endoscopic spectroscopy must be kept as short as possible because a change in the intensity during the measurement of a spectrum leads to distortion of the spectral response. For this reason, compared to the FTIR spectrometer, laser diodes are advantageous for the endoscopic system because they yield a considerably higher spectral power density and in principle allow a correspondingly shorter measuring time.

For clinical use of the endoscopic system changes in the position or of the bending radius of the wave guide connecting the endoscope with the spectrometer are unavoidable. The transmission of a wave guide depends on the bending radius of its geometrical configuration. As these values are only minimally dependent on the wavelength, their influence on the discriminant analysis can be almost entirely eliminated by normalisation of the spectra or by calculation of the intensity variant size.

6. Lead salt diode laser

IR laser diodes for the fibre supported endoscopic IR spectroscopy offer the following advantages compared to thermal radiation sources: (1) The spectral power density is higher due to the small bandwidth of its radiation. (2) Compared to the cross section area of the wave guide, the laser diode is a point-like radiation source. This means the coupling of the radiation is associated with relatively small losses which result from reflection losses at the fibre end surface and the aberration error of the incoupling optic. (3) The laser diode can be tuned by the current according to the wavelength as well as activation/deactivation which means that a rapid spectroscopic measurement is possible for a limited wavelength range without use of dispersive elements (grating) or interferometer. Biological tissue was measured in the wavenumber range 1000 cm^{-1}. Two lead salt laser diodes were operated in a laser module at electronically stabilised temperatures of 80–115 K and operating currents of up to 1 ampere. The maximum power output of the laser diodes used was 1 mW. A wavenumber range was selected corresponding to the microspectroscopic results at 1450 cm^{-1} and 1225 cm^{-1}. The wavelength of the laser radiation can be varied using either the temperature or the operating flow. The wavenumber range achieved by varying the current is maximally 50 cm^{-1}, at low operating currents at the activation threshold value of the laser diode, the laser power is considerably reduced and cannot used in spectroscopy. The threshold value for the application of the laser diode increases with increasing temperature and the tuning range decreases accordingly. At high temperatures or low working currents the laser operates in partial single mode operation ie the laser power is almost entirely delivered over a single resonator mode. A single mode operation cannot be attained for lead salt laser diodes for the entire operating current range. Operating currents over 0.6 A lead to a discontinuity in the laser power increase. Figure 19 shows

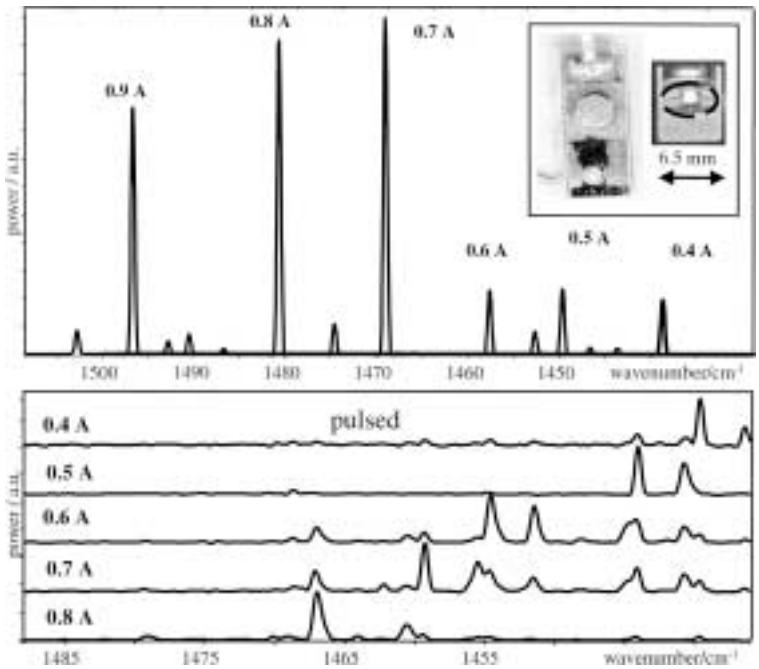

Fig. 19. Laser diode spectra ($T = 83.5$ K, current intensity $I_{\mathrm{LD}} = 0.4$ to 0.9 A). Above, the width of the line corresponds to the resolution of the spectrometer; inset, visible image of an IR laser diode, the active area is marked. Below, cyclic pulse operation, pulselength $t_{\mathrm{p}} = 1$ milliseconds.

laser diode spectra, which operate in mainly one mode over a wavenumber range of 60 cm^{-1} at temperatures of 83.5 K.

The laser module thermostat controls the temperature of the laser port to which the laser diode is attached. As the laser diode converts part of the delivered electrical energy into heat, a temperature gradient develops between the laser diode and the laser port. In the stationary condition (constant operating current), the corresponding temperature difference is proportional to the loss in power. In continuous wave (cw) mode the current modulation of the laser spectrum also indirectly affects a change in the diode temperature.

Turning on or changing the operating current intensity leads to a relaxation process in which the temperature distribution in the laser diode and laser port approaches the stationary condition. As the spectrum of the laser diode is highly sensitive to the temperature dependent, a corresponding relaxation process of the spectrum results. Measurements in multi-mode operation with a sensitive time resolution show that the relaxation process extends over a time frame of μsec to min. As the influence of the laser temperature is less for short current pulses, the tuned wavenumber range is smaller in pulsed mode (Fig. 19). Comparison of cw- and pulsed mode shows a reduction in the wavenumber range of 40 cm^{-1} to 25 cm^{-1}.

The properties of the laser diodes are subject to change with time due to the aging process. Even after a short time, (minutes) significant fluctuations in the laser spectrum was determined (not shown). As a result the entire spectroscopic system must include a regular calibration of the laser spectra. So far preliminary measurements were carried out using the experimental laboratory set-up in Fig. 20.

Both IR beams were superimposed after collimation with spherical concave mirrors. The signal of the detector was evaluated using a lock-in amplifier. The tissue sample was positioned below the fixed IR fibre using a motorised platform (resolution approx. 1 μm).

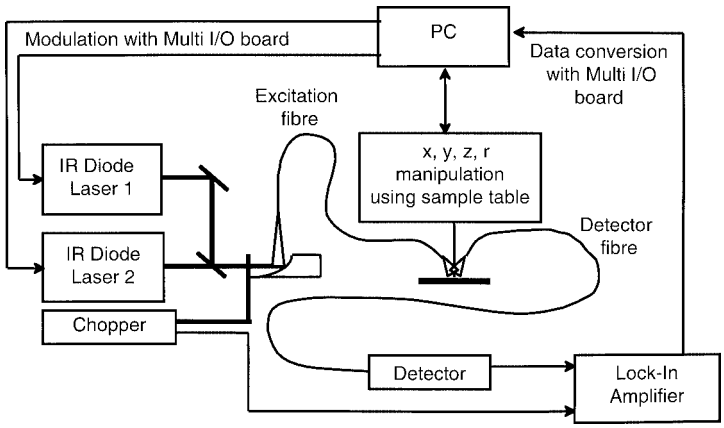

Fig. 20. Scheme of the IR fibre-optic experimental set-up.

7. Conclusion

Scattering affect were investigated using a bio-gel. The univariate method shows that the discriminance between different cell lines or tumour/healthy tissue is possible, even when restricted to two wavenumber regions for the colon tissue. However the method is susceptible to local disturbances of the spectra. IR sensors for ATR and reflection measurement were discussed.

For the IR-endospectroscopy with laser diodes resulted in the following requirements:

- *short measuring time*: In order to minimize the effect of movement of the instruments during the measuring time (i.e. the time taken for the absorption values to be acquired) this must be kept as short as possible.
- *low spectral resolution*: As the line widths in IR-tissue spectra are considerably larger than in gas phase spectra, the use of the modulations technique with lock-in technique (derivative spectroscopy) is not relevant.
- *measurement of several values of the spectrum in the tuning range of the laser diode.* Therefore a large tuning range of the laser diode is to prefer.
- *high signal/noise ratio*: For the discrimination of tumourous tissue in colon samples a value of $S/N > 1000$ is given.
- modulation of the laser diode with the temperature control (thermostat is not acceptable) for short measuring times because the adjustment times required are too long. Only a relatively small part of the band structure in a typical transmission spectrum of colon tissue can be recorded using the tuning range of a laser diode. Alternatively pulse modulation can be used which allows the rapid measurement of several sizes of the spectrum within the tuning range of the laser diode. This method is based on the cyclic modulation of laser diodes with a series of pulses with increasing current intensity I_{LD}.

Acknowledgements

This work was supported by the Senat of Berlin/European Community and the German Federal Ministry of Education and Research, Project. No.: 13N7064. The authors wish to thank Dr. med. Jörg Frege, Univ.-Hospital Benjamin Franklin, Freie University Berlin, Inst. of Pathology, for helpful discussion.

References

[1] M. Diem, S. Boydston-White and L. Chiriboga, Infrared spectroscopy of cells and tissues: shining light onto a novel subject, *Appl. Spectroscopy* **53** (1999), 148A–161A.
[2] M. Jackson, K. Kim, J. Tetteh, J.R. Mansfield, B. Dolenko, R.L. Somorjai, F.W. Ort, P.H. Watson and H.H. Mantsch, Cancer Diagnosis by Infrared Spectroscopy: Methodological Aspects, *SPIE* **3257** (1998), 24–34.
[3] S. Hocdé, C. Boussard-Plédel, G. Fonteneau and J. Lucas, Chalcogens based glasses for IR fiber chemical sensors, *Solid State Science* **3** (2001), 279–284.
[4] I.V. Scripachev, M.F. Churbanov, G.G. Devyatykh, E.M. Dianov and V.G. Plotnichenko, Chalcogenide glass infrared (CIR) fibers for process IR-spectroscopy and IR imaging in 1.5–6 mkm range, *SPIE* (2002), in press.
[5] J. Frank, R. Schindler, O. Lendl and B. Lendl, Improved fiber-detector coupling for MIR spectroscopy employing shaped silver halide fibers, *Appl. Spectroscopy* **54** (2000), 1417–1422.
[6] L. Küpper, H.M. Heise, F.-G. Bechara and M. Stücker, Micro-domain analysis of skin samples of moor-mummified corpses by evanescent wave infrared spectroscopy using silver halide fibers, *J. Molec. Struct.* **565–566** (2001), 497–504.
[7] U. Bindig, M. Meinke, I. Gersonde, O. Spector, I. Vasserman, A. Katzir and G. Müller, IR-Biosensor: flat silverhalide fiber for bio-medical sensing?, *Sensors and Actuators B* **74** (2001), 37–46.
[8] L. Küpper, H.M. Heise and L.N. Butvina, Novel developments in mid-IR fiber-optic spectroscopy for analytical applications, *J. Molec. Struct.* **563–564** (2002), 173–181.
[9] S. Hocde, O. Loreal, O. Sire, B. Turlin, C. Boussard-Pledel, D. Le Coq, B. Bureau, G. Fonteneau, C. Pigeon, P. Leroyer and J. Lucas, Biological tissue infrared analysis by chalcogenide glass optical fiber spectroscopy, *SPIE* **4158** (2001), 49–56.
[10] T. Uemura, K. Nishida, M. Sakakida, K. Ichinose, S. Shimoda and M. Shichiri, Non-invasive blood glucose measurement by Fourier transform infrared spectroscopic analysis through the mucous membrane of the lip: application of a chalcogenide optical fiber system, *Frontiers Med. Biol. Engng.* **9** (1999), 137–153.
[11] E. Bormashenko, R. Pogreb, S. Sutovski and M. Levin, Optical properties and infrared optics applications of composite films based on polyethylene and low-melting-point chalcogenide glass, *Opt. Eng.* **41** (2002), 295–302.
[12] E.D.S. Kerslake and C.G. Wilson, Pharmaceutical and biomedical applications of fiber optic biosensors based on infra red technology, *Advanced Drug Delivery Reviews* **21** (1996), 205–213.
[13] C.F. Baulsir and R.J. Simler, Design and evaluation of IR sensors for pharmaceutical testing, *Advanced Drug Delivery Reviews* **21** (1996), 191–203.
[14] V.G. Artjushenko, N.I. Afanasyeva, A. Lermann, A.P. Kryukov, E.F. Kuzin, N.N. Zharkova, V.G. Plotnichenko, G.A. Frank, G.I. Didenko and V.V. Sokolov, W. Neuberger, Medical applications of MIR-fiber spectroscopic probes, *SPIE* **2025** (1994), 137–142.
[15] Y. Gotshal, R. Simhi, B.-A. Sela and A. Katzir, Blood diagnostics using fiberoptic evanescent wave spectroscopy and neural networks analysis, *Sensors and Actuators B* **42** (1997), 157–161.
[16] N.I. Afanasyeva, S. Kolyakov and L.N. Butvina, Remote skin tissue diagnostics in vivo by fiber optic evanescent wave Fourier transform infrared (FEW-FTIR) spectroscopy, *SPIE* **3257** (1998), 260–266.
[17] R.F. Bruch, S. Sukuta, N.I. Afanasyeva, S.F. Kolyakov and L.N. Butvina, Fourier transform infrared evanescent wave (FTIR-FEW) spectroscopy of tissue, *SPIE* **2970** (1997), 408–415.
[18] A. Brooks, R.F. Bruch, N.I. Afanasyeva, S.F. Kolyakov, L.N. Butvina and L. Ma, Investigations of normal human skin tissue and acupuncture points of human skin tissue using fiberoptical FTIR spectroscopy, *SPIE* **3262** (1998), 173–184.
[19] J.-G. Wu, Y.-Z. Xu, C.-W. Sun, R.D. Soloway, D.-F. Xu, Q.-G. Wu, K.-H. Sun, S.-F. Weng and G.-X. Xu, Distinguishing malignant from normal oral tissues using FTIR fiber-optic techniques, *Biopolymers* **62** (2001), 185–192.
[20] S.-F. Weng, X.-F. Ling, Y.-Y. Song, Y.-Z. Xu, W.-H. Li, X. Zhang, L. Yang, W. Sun, X. Zhou and J. Wu, FTIR fiber optics and FT–Raman spectroscopic studies for the diagnosis of cancer, *Am. Clin. Lab.* **19** (2000), 20.
[21] D. Bunimovich, R. Kellner, R. Krska, A. Mesica, I. Paiss, U. Schiesl, M. Tacke, K. Taga and A. Katzir, A system for monitoring & control of processes based on IR Fibers and tunable diode laser, *J. Molec. Struct.* **292** (1993), 125–132.
[22] P. Werle, F. Slemr, K. Maurer, R. Kormann, R. Mücke and B. Jänker, Near- and mid-infrared laser-optical sensors for gas analysis, *Optics and Laser in Engineering* **37** (2002), 101–114.
[23] Genetic-algorithm routines developed by David L. Carroll at the University of Illinois have been used. For an introduction see: D.E. Goldberg, *Genetic Algorithms in Search, Optimization and Machine Learning*, Addision-Wesley, 1989.
[24] K.V. Mardia, J.T. Kent and J.M. Bibby, *Multivariate Analysis*, Academic Press, London, 1979.
[25] S. Sukuta and R. Bruch, Factor analysis of cancer fourier transform infrared evanescent wave fiberoptical (FTIR-FEW) spectra, *Lasers in Surgery and Medicine* **24** (1999), 382–388.
[26] S. Argov, J. Ramesh, A. Salman, I. Sinelnikov, J. Goldstein, H. Guterman and S. Mordechai, Diagnostic potential of Fourier-transform infrared microspectroscopy and advanced computational methods in colon cancer patients, *J. Biomed. Optics* **7** (2002), 248–254.
[27] J.A. Harrington, A review of IR transmitting hollow waveguides, *Fiber and Integrated Optics* **19** (2000), 211–217.

[28] E. Bormashenko, R. Pogreb, S. Sutovski, I. Vaserman and A. Katzir, The use of polymer coated AgClBr fibers for fiberoptic evanescent wave spectroscopy (FEWS) of biological fluids, *SPIE* **3570** (1999), 100–106.
[29] J. Reichlin, E. Bormashenko, A. Sheshnev, R. Pogreb, E. Shulzinger and A. Katzir, Investigation of water penetration in polystyrene by use of polymer-coated AgClBr-fibers and development of new sensor intended for the FEWS spectroscopy of organic compounds in water, *SPIE* **4129** (2000), 305–313.